Eidgenössische Technische Hochschule Zürich
Swiss Federal Institute of Technology Zurich

Shape Sensitivity in 2D Acoustic Scattering

Bachelor Thesis

Moa Sjöberg

msjoeberg@ethz.ch

Department of Mathematics
ETH Zürich

Supervisor:
Prof. Dr. Ralph Hiptmair

May 30, 2023

Abstract

In this thesis, we deal with shape sensitivity in 2D acoustic scatter. More precisely, we are dealing with an inverse scattering problem as a shape optimization problem, where we define a functional J which measures the difference between the given measured data and the computed solution, the goal is then to find the shape that minimizes the functional.

The focus in this thesis lies on computing the derivative of J which is relevant when investigating shape sensitivity. The derivative will be computed with a method called the adjoint method. Lastly, we will introduce the method of fundamental solution. Here, the scattered wave is approximated using the fundamental solution of the Helmholtz equation, and the shape-derivative J will be computed considering the approximation.

Contents

Abstract **i**

1 Introduction **1**

1.1 Definitions 1

1.2 The Acoustic Problem 2

2 Acoustic Model **6**

2.1 Harmonic signals 6

2.2 Wave equation and Helmholtz equation 6

2.2.1 Sound-soft and Sound-hard Obstacles 7

2.2.2 Sommerfeld Radiation Condition 7

2.3 Green's theorem and formula 8

2.4 The Far-field Pattern 9

2.4.1 Far-field Pattern as a Volume Integral 10

3 Derivation of the Shape-Gradient **15**

3.1 The Shape-gradient 15

3.1.1 Shape Function 15

3.1.2 Shape Gradient 15

3.2 Derivative of the Shape Gradient 16

3.3 Adjoint method 16

4 The Method of Fundamental Solution **24**

4.1 The Method of Fundamental Solutions for scattering problems . . 24

4.1.1 Structure of algorithm in 2D 25

4.2 Inverse Scattering problem with MFS 30

5 Conclusion and Outlook **33**

Bibliography **34**

A Source Code **A-1**

A.1 Numerical example A-1

A.1.1 Least square solution of **c** A-1

A.1.2 Plots of the scattered wave A-2

A.2 Plot of Hankel function A-5

Chapter 1

Introduction

The term "shape sensitivity" describes how an object's shape or geometry affects a functional output, such as a cost or performance metric. It is frequently employed in the field of optimization, where the objective is to identify an object's ideal shape while satisfying a set of performance requirements. It is feasible to build more efficient methods by understanding how changes of the shape impact the functional output. Numerous systems, including aerodynamic designs, vehicle structures, and medical devices, can be improved using shape sensitivity. Shape sensitivity is a powerful tool for engineers wanting to create innovative and efficient products.

In this work, the focus lies on shape sensitivity of acoustic scattering. Acoustic scattering is the process by which sound waves are scattered by objects. When sound waves encounter an object, they can be absorbed, transmitted, or scattered in different directions, depending on the size, shape, and composition of the object. Acoustic scattering is an important phenomenon in various fields, such as underwater acoustics, sonar imaging and medical ultrasound. By analyzing the scattered sound waves, it is possible to obtain information about the size, shape, and position of the object that caused the scattering.

In our scenario, a planar wave is scattered by a long object in a two-dimensional environment and the translation is invariant in one direction. The initial object from which the sound waves were scattered by, can be found with the aid of inverse problem optimization. To do that, we want to compute the shape derivative. However, we firstly state some relevant definition and the problem setting will be defined and explained in Chapter 1 and 2.

1.1 Definitions

Definition 1.1. (Vector-field)([1], Ch. 2) A vector-field $\mathcal{X}$ on $U \subset \mathbb{R}^n$ is a function which assigns to each of the points U a vector at that point p. Thus,

$$\mathcal{X}(p) = (p, X(p)),$$

for some function $X : U \to \mathbb{R}^n$.

Definition 1.2. (Hankel function)([2], Sect. 2.3, Ch.2) We call

$$H_n^1(z) = J_n(z) + Y_n(z)$$

the first Hankel function of order n, where

$$J_n(z) = \frac{z}{n} \sum_{j=1}^{\infty} \frac{\left(-\frac{z^2}{a}\right)}{j!(n+j)!}$$

is the Bessel function of the first kind and $Y_n(z)$ the Bessel function of the second kind for all series of H_n^1. In figure 1.1 you can see a plot of the real and imaginary parts of H_n^1. As r increases, the real part oscillates around zero, demonstrating the Bessel function of the first kind. It has a zero crossing at a certain point. The imaginary part also oscillates, but is out of phase with the real part. It has the same zero crossings as the real part but shifted in phase by $\pi/2$.

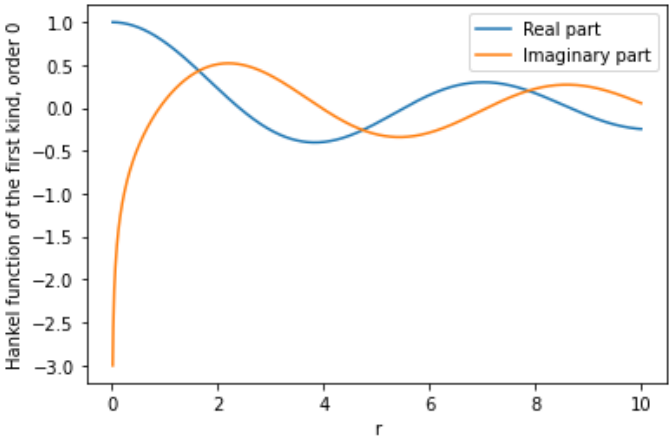

Figure 1.1: Real and Imaginary part of H_0^1

Definition 1.3. In this work the linear space $H_{\partial D}^1(\Omega)$ is given by:

$$H_{\partial D}^1(\Omega) = \{w \in H^1(\Omega) : w|_{\partial D} = 0\}. \tag{1.1}$$

1.2 The Acoustic Problem

Let $D \in \mathbb{R}^2$ be a bounded simply connected planar domain with analytic boundary such that $\Omega := \mathbb{R}^2 \setminus \bar{D} \in \mathbb{R}^2$ is connected. Besides that, we are given a wave number $k > 0 \in \mathbb{R}^2$ and an incoming wave

$$u_{inc} = e^{ikd \cdot x},$$

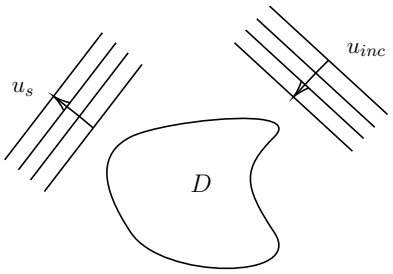

Figure 1.2: Acoustic scattering

moving in the unit direction $d = \{d \in \mathbb{R}^2 : |d| = 1\}$. The scatterer of u_{inc} produces a scattered wave u_s, where the total wave is

$$u = u_{inc} + u_s$$

Acoustic waves, satisfy the wave equation. The time harmonic solution of the wave equation satisfies the Helmholtz equation. Furthermore, we are considering a sound-soft obstacle with Dirchlet boundary condition.

Thereby, the boundary value problem corresponding to the acoustic problem is given by the *state equation*:

$$\begin{cases} \Delta u + k^2 u = 0 & \text{in } \Omega \\ u = 0 & \text{on } \partial D \end{cases} \tag{1.2}$$

$$\lim_{\mathbf{r}\to\infty} \sqrt{\mathbf{r}}\,(\partial_{\mathbf{r}}(u_s) - iku_s) = 0. \tag{1.3}$$

It is also required that the waves satisfy the Sommerfeld radiation condition (1.2), which guarantees that the wave is outgoing when going towards infinity.

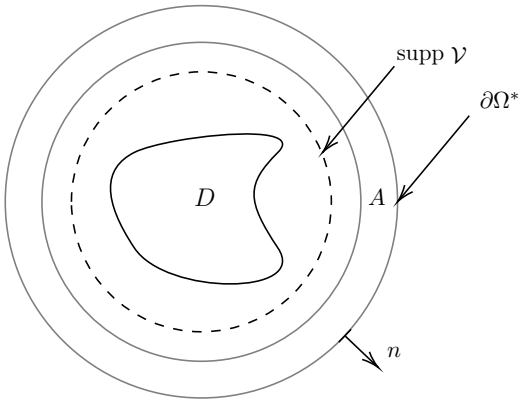

Figure 1.3: Geometrical Setting

Geometrical setting

The geometrical setting consists of a scatterer, a long shape $D \in \mathbb{R}^2$, which is affected by shape variation effected by a deformation vector-field. We also consider a circular strip A, that does not undergo deformation by the vector-field. This is the integration domain of the far-field function that will be introduced in the next chapter. The measured data $u_g \in L^2(\mathbb{S}^1)$ is given. The truncation boundary $\partial\Omega^*$ is a smooth artificial boundary enclosing the scatterer. Lastly, we have that $\mathbf{n}$ is the unit normal vector of the truncation boundary $\partial\Omega^*$.

Variational formulation

To simplify computations, we will derive a weak formulation of (1.2). This formulation involves replacing the strong form of the equation, which is based on derivatives, with an equivalent integral form that is based on integrals and functions. The new formulation is going to become helpful later, when deriving the shape-derivative.

Theorem 1.4 (Variational formulation)**.** *The variational formulation of the boundary conditions in (1.2) can be formulated as:*

Seek $u \in H^1_{\partial D}(\Omega) = \{w \in H^1(\Omega) : w|_{\partial D} = 0\}$*, such that*

$$a(u, v) = l(v) \tag{1.4}$$

for all $v \in H^1_{\partial D(\Omega)}$*.* $a(u, v)$ *and* $l(v)$ *are defined as follows:*

$$\begin{aligned} a(u, v) &= \int_{\Phi_s(\Omega)} -\nabla(u) \cdot \nabla(v) - k^2 uv dx + \int_{\partial\Omega^*} Dt\mathcal{N}_k(u|_{\partial\Omega^*})v|_{\partial\Omega^*} dS, \\ l(v) &= \int_{\partial\Omega^*} (-\gamma_N u_{inc} + Dt\mathcal{N}_k(u_{inc}|_{\partial\Omega^*}))v|_{\partial\Omega^*} dS, \end{aligned} \tag{1.5}$$

and where $\partial\Omega^*$ *is the truncation boundary,* $Dt\mathcal{N}_k$ *is a Dirchlet-to-Neumann-operator, defined as* $\nabla(u) \cdot \mathbf{n} = Dt\mathcal{N}_k(u)$ *and* $\gamma_N u^{inc} = u \cdot \mathbf{n}|_{\partial\Omega^*}$ *the Neumann trace.*

Proof. The boundary condition (1.2) implies that the following holds:

$$\begin{aligned} & \int_\Omega (\mathrm{div}\nabla u + k^2 u)v dx = 0 \quad \forall v \in C^\infty(\bar{\Omega}) \text{ and } v|_{\partial D} = 0 \\ \rightarrow \quad & \int_\Omega -\nabla u \cdot \nabla v + k^2 uv dx + \int_{\partial\Omega^*} (\nabla u \cdot \mathbf{n})v dS = 0. \end{aligned}$$

The implication follows straightforwardly through integration by parts. Next, we use the following notation $\nabla(u - u_{inc}) \cdot \mathbf{n} = Dt\mathcal{N}_k(u - u_{inc}|_{\partial\Omega^*})$, and $\gamma_N u^{inc} = u \cdot \mathbf{n}|_{\partial\Omega^*}$. This gives together with $Dt\mathcal{N}_k$ being linear,

$$\int_\Omega -\nabla u \cdot \nabla v + k^2 uv dx + \int_{\partial\Omega^*} Dt\mathcal{N}_k(u|_{\partial\Omega^*}) + \underbrace{\nabla u_{inc} \cdot \mathbf{n}}_{\gamma_N u_{inc}} - Dt\mathcal{N}_k(u_{inc}|_{\partial\Omega^*}) dS = 0.$$

Moving the last two terms in the last integral to the right-hand side yields (1.4). □

We have now covered the idea of form sensitivity and its application to optimization. In this Chapter, the direct exterior scattering problem has been presented as well as the problem's variational formulation, supplying the groundwork for deriving the shape derivative. In the next chapter, we will introduce the acoustic model and introduce the far-field pattern.

Chapter 2

Acoustic Model

Although this paper focuses on shape sensitivity, we are going to give a brief description of sound and its behavior. For most people, sound is synonymous to hearing. But in fact sound is acoustic waves which describe the fluctuation of pressure([3] Sect. 1.0, Ch. 1). In the end, we are going to introduce the far-field and derive a volume representation formula, which is useful when defining the shape function and deriving the derivative in Chapter 3.

2.1 Harmonic signals

The basic mathematical description of a harmonic signals can be written as a sine or a cosine wave in time,

$$p(t) = A\cos(\omega t + \phi_s) \text{ or } p(t) = A\sin(\omega t + \phi_c). \tag{2.1}$$

The parameter A is the amplitude. The term ω is used to referring to the circular frequency, $\omega = \frac{2\pi}{T}$, where the period in which each pattern repeats is referred to as T.

A more convenient way to work with harmonic signals is by using the complex representation

$$Ae^{ik\cdot\mathbf{x}} = A\cos(\omega t) + iA\sin(\omega t).$$

([3] Sect. 1.1, Ch. 1)

2.2 Wave equation and Helmholtz equation

In this section, we will give a short introduction to what acoustic waves are, as well as their behavior and properties. For this, we follow Colton and Kress's book ([4] Sect. 2.1, Ch. 2) if not stated otherwise.

We consider the propagation of soundwaves to be amplitudes in a homogenous isotropic medium in space and the motion is determined by the linearized wave equation

$$\frac{1}{c^2}\frac{\partial^2 U}{\partial t^2} = \Delta U, \tag{2.2}$$

where $U = U(x,t)$ is the scalar time-dependent velocity potential depending on the particle's velocity field. Moreover, c is the acoustic speed. For time-harmonic acoustic waves of the form

$$U(x,t) = \mathrm{Re}\{u(x)e^{-i\omega t}\}, \tag{2.3}$$

where $\omega > 0$ is the angular frequency, we obtain the Helmholtz equation when substituting (2.3) into the wave equation (2.2)

$$\Delta u + k^2 u = 0,$$

where k represents the wave number. Therefore, time-harmonic acoustic waves can be modeled with the Helmholtz equation.

2.2.1 Sound-soft and Sound-hard Obstacles

In obstacle scattering it is important to differentiate between penetrable and impenetrable objects, also called sound-soft and sound-hard obstacles.

For a sound-soft obstacle, the total pressure vanishes on the boundary of the obstacle. More precisely, let us consider the scattering of an incoming wave u^i by a sound-soft object D. Then the total wave $u = u^i + u^s$ consisting of the sum of the incoming wave and the scattered wave, must satisfy not only the wave equation in the exterior $\mathbb{R}^2 \setminus \bar{D}$ but also the Dirichlet boundary condition $u = 0$ on ∂D

On the other hand, for sound-hard obstacles, as the normal velocity of the acoustic wave vanishes on the boundary, we get a Neumann boundary condition $\frac{\partial u}{\partial \mathbf{n}} = 0$ on ∂D where $\mathbf{n}$ is the unit outward normal of the boundary.

In this work, we are only considering a sound-soft obstacle D.

2.2.2 Sommerfeld Radiation Condition

To ensure uniqueness for the scattered wave, u_s Sommerfeld introduced the radiation condition

$$\lim_{\mathbf{r}\to\infty} \sqrt{\mathbf{r}}\,(\partial_{\mathbf{r}}(u_s) - iku_s) = 0, \tag{2.4}$$

where $\mathbf{r} = |\mathbf{x}|$ [5]. (This is the radiation conditions for the two-dimensional case). It is worth noting that only the first one, of the following possible spherically symmetric solutions

$$\frac{e^{ik|\mathbf{x}|}}{|\mathbf{x}|} \text{ and } \frac{e^{-ik|\mathbf{x}|}}{|\mathbf{x}|}$$

of the Helmholtz equation satisfies the radiation condition. Physically, the Sommerfeld radiation condition guarantees that it is an outgoing wave.

2.3 Green's theorem and formula

In this section we follow Colton and Kress's book ([4] Sect. 2.2, Ch. 2).

Most of the solutions to the Helmholtz equation $\Delta u + k^2 u = 0$ can be deduced from the fundamental solution

$$\Phi_k(\mathbf{x}) = \frac{i}{4} H_0^{(1)}(k|\mathbf{x} - \mathbf{y}|), \ \mathbf{x} \neq \mathbf{y}$$

(This is the fundamental solution in the two-dimensional case). Straight-forward differentiation shows that it satisfies the Helmholtz equation in $\mathbb{R}^2 \setminus \{\mathbf{y}\}$.

One important basic tool in the study of the Helmholtz equation is provided by Green's integral theorems.

Theorem 2.1. *(Green's Theorem) Let D be a bounded domain of class C^1 and let $\mathbf{n}$ denote the unit normal vector to the boundary ∂D directed into the exterior of D. Then, for $u \in C^1(\bar{D})$ and $v \in C^2(\bar{D})$ we have Green's first theorem*

$$\int_D (u\Delta v + \nabla u \cdot \nabla v) dx = \int_{\partial D} u \frac{\partial v}{\partial \mathbf{n}} ds, \tag{2.5}$$

and for $u, v \in C^2(\bar{D})$ we have Green's second theorem

$$\int_D (u\Delta v - v\Delta u) dx = \int_{\partial D} \left(u \frac{\partial u}{\partial \mathbf{n}} - v \frac{\partial u}{\partial \mathbf{n}} ds \right). \tag{2.6}$$

With help of the Green's theorem, the following theorem can be derived.

Theorem 2.2. [1] *Assume the bounded set D is the open complement of an unbounded domain of class C^2 and let $\mathbf{n}$ denote the unit normal vector to the boundary ∂D directed to the exterior of D. Let $u \in C^2(\mathbb{R}^2 \setminus D) \cap C(\mathbb{R}^2 \setminus D)$ be a radiating solution to the Helmholtz equation*

$$\Delta u + k^2 u = 0 \text{ in } \mathbb{R}^2 \setminus \bar{D},$$

[1] The Theorem is taken from ([4] Sect. 2.2, Ch. 2, Thm 2.2).

which possesses a normal derivative on the boundary in the sense that the limit

$$\frac{\partial u}{\partial \mathbf{n}}(\mathbf{x}) = \lim_{h \to +0} (\mathbf{x}) \cdot \nabla u(\mathbf{x} + h\mathbf{n}),\ \mathbf{x} \in \partial D$$

exists uniformly on ∂D. Then we have Green's formula,

$$u(\mathbf{x}) = \int_{\partial D} \left\{ u(\mathbf{y}) \frac{\partial \Phi(\mathbf{x}, \mathbf{y})}{\partial \mathbf{n}(\mathbf{y})} - \frac{\partial u}{\partial \mathbf{n}}(\mathbf{y}) \Phi(\mathbf{x}, y) \right\} ds(\mathbf{y}) - \int_D \left\{ \Delta u(\mathbf{y}) + k^2 u(\mathbf{y}) \right\} \Phi(\mathbf{x}, \mathbf{y}),\ \mathbf{x} \in \mathbb{R}^2 \setminus \bar{D},$$

where the volume integral exists as an improper integral. However, as u is a solution of the Helmholtz equation

$$\Delta u + k^2 u = 0 \text{ in } \mathbb{R}^2 \setminus \bar{D},$$

the second term vanishes, and we are left with the following Green's representation formula of $u(x)$:

$$u(\mathbf{x}) = \int_{\partial D} \left\{ u(\mathbf{y}) \frac{\partial \Phi(\mathbf{x}, \mathbf{y})}{\partial \mathbf{n}(\mathbf{y})} - \frac{\partial u}{\partial \mathbf{n}}(\mathbf{y}) \Phi(\mathbf{x}, \mathbf{y}) \right\} ds(\mathbf{y}),\ \mathbf{x} \in \mathbb{R}^2 \setminus \bar{D}. \tag{2.7}$$

2.4 The Far-field Pattern

The radiation condition leads to an asymptotic behavior of the scattered wave. More precisely, we have the following theorem.

Theorem 2.3. [2] *Every radiating solution u to the Helmholtz equation has the asymptotic behavior of an outgoing wave*

$$u(\mathbf{x}) = \frac{e^{ik|\mathbf{x}|}}{\sqrt{|\mathbf{x}|}} \left\{ u_\infty(\hat{\mathbf{x}}) + \mathcal{O}\left(\frac{1}{|\mathbf{x}|} \right) \right\},\ |\mathbf{x}| \to \infty \tag{2.8}$$

uniformly in all directions, $\hat{\mathbf{x}} = \frac{\mathbf{x}}{|\mathbf{x}|}$, where the function u_∞ defined on the unit circle $\mathbb{S}^1$ is known as the far-field pattern of u. Under the assumption of Theorem (2.2) we have

$$u_\infty(\hat{\mathbf{x}}) = \frac{1}{4\pi} \int_{\partial D} \left\{ u(\mathbf{y}) \frac{\partial \Phi^\infty(\hat{\mathbf{x}}, \mathbf{y})}{\partial \mathbf{n}(\mathbf{y})} - \frac{\partial u}{\partial \mathbf{n}}(\mathbf{y}) \Phi^\infty(\hat{\mathbf{x}}, \mathbf{y}) \right\} dS(y), \tag{2.9}$$

where $\Phi^\infty(\hat{\mathbf{x}}, \mathbf{y})$ satisfies the asymptotic behavior

$$\Phi(\mathbf{x}, \mathbf{y}) = \frac{e^{ik|\mathbf{x}|}}{\sqrt{|\mathbf{x}|}} \left(\Phi^\infty(\hat{\mathbf{x}}, \mathbf{y}) + \mathcal{O}\left(\frac{1}{|\mathbf{x}|} \right) \right) \text{ for } \mathbf{x} \to \infty. \tag{2.10}$$

[2] The theorem is taken from ([4] Sect. 2.2, Ch. 2, Thm 2.6), and adapted for the two-dimensional case.

Example 2.4. In the two-dimensional case, we have that

$$\Phi_k(\mathbf{r}) = \frac{i}{4} H_0^{(1)}(k|\mathbf{x}-\mathbf{y}|),\ \mathbf{x} \neq \mathbf{y},$$

where $H_0^{(1)}$ is the Hankel function. The asymptotics of the Hankel function is

$$H_0^{(1)}(\mathbf{r}) = \sqrt{\frac{2}{\pi \mathbf{r}}} \cdot e^{i(\mathbf{r}-\frac{\pi}{4})} + \mathcal{O}(\mathbf{r}^{-\frac{3}{2}}) \text{ for } \mathbf{r} \to \infty,$$

[6]. Now if we keep $\mathbf{y}$ fixed and let $|\mathbf{x}| \to \infty$, we obtain the following behavior of $(\mathbf{x}, \mathbf{y}) \mapsto \Phi(\mathbf{x}, \mathbf{y})$.

$$\begin{aligned}
\Phi(\mathbf{x},\mathbf{y}) &= -\frac{i}{a} H_0^1 \left(k \left(|\mathbf{x}| - \hat{\mathbf{x}} \cdot \mathbf{y} + \mathcal{O}\left(\frac{1}{|\mathbf{x}|}\right)\right)\right) \\
&= -\frac{i}{4} \sqrt{\frac{2}{\pi k \left(|\mathbf{x}| - \hat{\mathbf{x}} \cdot \mathbf{y} + \mathcal{O}\left(\frac{1}{|\mathbf{x}|}\right)\right)}} e^{ik\left(|\mathbf{x}| - \hat{\mathbf{x}}\cdot\mathbf{y} + \mathcal{O}\left(\frac{1}{|\mathbf{x}|}\right)\right) - \frac{i\pi}{4}} + \mathcal{O}(|\mathbf{x}|^{-\frac{3}{2}}) \\
&\quad \text{Note: For the next equality, we use the fact that } (1+t)^{-\frac{1}{2}} = 1 - \frac{1}{2}t + \mathcal{O}(t^2) \\
&= -\frac{i}{4}\sqrt{\frac{2}{\pi k}} \frac{e^{ik|\mathbf{x}| - i\frac{\pi}{4}}}{\sqrt{|\mathbf{x}|}} \left(1 - \frac{1}{2}\hat{\mathbf{x}} \cdot \frac{\mathbf{y}}{|\mathbf{x}|} + \mathcal{O}(|x|)^{-2}\right) e^{-ik\hat{\mathbf{x}}\cdot\mathbf{y}} \left(1 + \mathcal{O}\left(\frac{1}{|\mathbf{x}|}\right) + \mathcal{O}(|\mathbf{x}|)^{-\frac{3}{2}}\right) \\
&= \frac{e^{ik|\mathbf{x}|}}{\sqrt{|\mathbf{x}|}} \left(\underbrace{-\frac{i}{4}\sqrt{\frac{2}{\pi k}} e^{-i\frac{\pi}{4}} e^{-ik\hat{\mathbf{x}}\cdot\mathbf{y}}}_{\Phi^\infty(\hat{\mathbf{x}},\mathbf{y})} + \mathcal{O}\left(\frac{1}{|\mathbf{x}|}\right)\right).
\end{aligned}$$

We can therefore conclude that

$$\Phi^\infty(\hat{\mathbf{x}}, \mathbf{y}) = -\frac{1}{\sqrt{k}} \frac{e^{i\frac{\pi}{4}}}{2\sqrt{2\pi}} e^{-ik\hat{\mathbf{x}}\cdot\mathbf{y}}.$$

Remark 2.5. It turns out that $\Phi^\infty(\hat{\mathbf{x}}, \mathbf{y}) = C_{d,k} e^{-ik\hat{\mathbf{x}}\cdot\mathbf{y}}$ holds in any dimension, with $C_{d,k}$ a constant depending on the dimension d and the wave number k.

2.4.1 Far-field Pattern as a Volume Integral

The far-field pattern can alternatively be expressed as a volume integral, which we show in the following theorem:

Theorem 2.6. *The far-field pattern (2.9) can be rewritten as a volume integral*

$$u^{\infty}(\hat{\mathbf{x}}) = C_{d,k} \int_A (\Delta\Psi - ik\hat{\mathbf{x}}\nabla\Psi) e^{-k\hat{\mathbf{x}}\cdot\mathbf{y}} u(\mathbf{y}) d\mathbf{y}, \tag{2.11}$$

with $C_{d,k} = \frac{1}{\sqrt{k}} \frac{e^{i\frac{\pi}{4}}}{2\sqrt{2\pi}}$ *in the 2-dimensional case, and* $\Psi \in C^2(\mathbb{R}^2)$ *being a cut-off function satisfying:*

- $0 \leq \Psi(\mathbf{x}) \leq 1$,
- $\operatorname{supp}\Psi \cap \bar{D} = \emptyset$,
- $\Psi = 1$ *for* $|\mathbf{x}| > R_1$.

Proof. We start with Green's representation formula (2.7) of any solution u of the Helmholtz equation, where $\Phi(\mathbf{x}, \mathbf{y})$ is the fundamental solution of the Helmholtz equation.

From *Theorem* 2.2, we have that the following holds:

$$\begin{aligned} u(\mathbf{x}) = &\int_{\partial D} \left\{ u(\mathbf{y}) \frac{\partial \Phi(\mathbf{x}, \mathbf{y})}{\partial \mathbf{n}(\mathbf{y})} - \frac{\partial u}{\partial \mathbf{n}}(\mathbf{y}) \Phi(\mathbf{x}, \mathbf{y}) \right\} dS(\mathbf{y}) \\ &- \int_D \Phi(\mathbf{x}, \mathbf{y}) (\Delta + k^2) u(\mathbf{y}) d\mathbf{y}, \end{aligned} \tag{2.12}$$

where D is the bounded open complement of an unbounded domain of class C^2. Now let u solve

$$(\Delta + k^2)u = 0 \text{ for } |\mathbf{x}| \geq R_0$$

as well as the Sommerfeld condition (2.4). Then pick a cut-off function $\Psi \in C^2$ such that

$$\begin{aligned} &\Psi(x) = 0 \text{ for } |\mathbf{x}| \leq R_0 \\ &\Psi(x) = 1 \text{ for } |\mathbf{x}| > R_1 > R_0. \end{aligned} \tag{2.13}$$

Set $\omega = \Psi u$. With the product rule and the fact that $(\Delta + k^2)u = 0$ for $|\mathbf{x}| \geq R_0$, it holds that

$$\begin{aligned} (\Delta + k^2)\omega &= 2\nabla\Psi \cdot \nabla u + u\Delta\Psi + \underbrace{\Psi(\Delta + k^2)u}_{=0} \\ &= 2\nabla\Psi \cdot \nabla u + u\Delta\Psi. \end{aligned} \tag{2.14}$$

Now before continuing we will derive the following lemma:

Lemma 2.7.

$$\int_{|\mathbf{x}|=R} \left\{ u(\mathbf{y}) \frac{\partial \Phi(\mathbf{x}, \mathbf{y})}{\partial \mathbf{n}(\mathbf{y})} - \frac{\partial u(\mathbf{y})}{\partial \mathbf{n}} \Phi(\mathbf{x}, \mathbf{y}) \right\} dS(\mathbf{y}) = 0 \quad \textit{for } R \to \infty.$$

Proof of Lemma. We first show that

$$\int_{|\mathbf{x}|=R} |u|^2 dS(\mathbf{y}) = \mathcal{O}(1), \quad \text{for } R \to \infty \tag{2.15}$$

To do this, we first notice that from the radiation condition the following holds:

$$\int_{|\mathbf{x}|=R} \left\{ \left| \frac{\partial u}{\partial \mathbf{n}} \right|^2 + k^2 |u|^2 + \text{Im}\left(u \frac{\partial \bar{u}}{\partial \mathbf{n}} \right) \right\} dS(\mathbf{y}) = \int_{|\mathbf{x}|=R} \left| \frac{\partial u}{\partial \mathbf{n}} - iku \right|^2 dS(\mathbf{y}) \to 0, \quad R \to \infty,$$

where $\mathbf{n}$ is the unit outwards normal to R. We now choose R big enough such that $\bar{D}$ is contained in the circle with radius R. Then by applying *Green's Theorem* (2.1) on the domain $D_R := \{y \in \mathbb{R}^2 \setminus \bar{D} : |y| < R\}$ we obtain

$$\int_{D_R} \Delta u \bar{u} + \nabla u \nabla \bar{u} d\mathbf{y} = \int_{\partial D_R} u \frac{\partial \bar{u}}{\partial \mathbf{n}} dS(\mathbf{y}). \tag{2.16}$$

Together with the fact that $(\Delta + k^2)u = 0$ for $|\mathbf{x}| \in \mathbb{R}^2 \setminus \bar{D}$ and $S_R := \{x \in \mathbb{R}^2 : |x| = R\} = \partial D_R \setminus \partial D$ we obtain

$$\int_{|\mathbf{x}|=R} u \frac{\partial \bar{u}}{\partial \mathbf{n}} dS(\mathbf{y}) = -\int_{\partial D} u \frac{\partial \bar{u}}{\partial \mathbf{n}} dS(\mathbf{y}) - k^2 \int_{D_R} |u|^2 d\mathbf{y} + \int_{D_R} |\nabla u|^2 d\mathbf{y} \tag{2.17}$$

By inserting the imaginary part of (2.17) into (2.16) we find that

$$\lim_{R\to\infty} \int_{|\mathbf{x}|=R} \left\{ \left| \frac{\partial u}{\partial \mathbf{n}} \right|^2 + k^2 |u|^2 \right\} dS(\mathbf{y}) = 2k \text{ Im} \int_{\partial D} u \frac{\partial \bar{u}}{\partial \mathbf{n}} dS(\mathbf{y}). \tag{2.18}$$

Both terms on the right-hand side of (2.18) are non-negative, and the left-hand side equals zero as $u = 0$ on ∂D. Therefore, each term on the right-hand side must individually be bounded as $R \to \infty$. Therefore, (2.15) must hold.

Now with (2.15), the Sommerfeld's radiation for $(x, y) \to \Phi(x, y)$

$$\frac{\partial \Phi(\mathbf{x}, \mathbf{y})}{\partial \mathbf{n}} - ik\Phi(\mathbf{x}, \mathbf{y}) = \mathcal{O}\left(\frac{1}{\mathbf{r}} \right), \quad R \to \infty, \tag{2.19}$$

and the Cauchy-Schwartz inequality $\langle \mathbf{a}, \mathbf{b} \rangle \leq ||\mathbf{a}|| \cdot ||\mathbf{b}||$ for $\mathbf{a}, \mathbf{b} \in \mathbb{R}^2$, we get:

$$I_1 = \int_{|\mathbf{x}|=R} u(\mathbf{y}) \left\{ \frac{\partial \Phi(\mathbf{x}, \mathbf{y})}{\partial \mathbf{n}(\mathbf{y})} - ik\Phi(\mathbf{x}, \mathbf{y}) \right\} dS(\mathbf{y}) \to 0, \quad R \to \infty. \tag{2.20}$$

Together with the radiation condition (1.3) for u and $\Phi(\mathbf{x}, \mathbf{y}) = \mathcal{O}(\mathbf{r}^{-\frac{3}{2}})$ (follows from the asymptotics of the Hankel function, see *Example* 2.4) for $\mathbf{y} \in S_R$, we get

$$I_2 = \int_{|\mathbf{x}|=R} \Phi(\mathbf{x}, \mathbf{y}) \left\{ \frac{\partial u}{\partial \mathbf{n}}(\mathbf{y}) - iku(\mathbf{y}) \right\} dS(\mathbf{y}) \to 0, \quad R \to \infty. \tag{2.21}$$

Therefore,

$$\int_{|\mathbf{x}|=R} \left\{ u(\mathbf{y}) \frac{\partial \Phi(\mathbf{x},\mathbf{y})}{\partial \mathbf{n}(\mathbf{y})} - \frac{\partial u(\mathbf{y})}{\partial \mathbf{n}} \Phi(\mathbf{x},\mathbf{y}) \right\} dS(\mathbf{y}) = I_1 - I_2 = 0 \quad \text{for } R \to \infty.$$

□

Besides Lemma 2.7 we also have that,

1. $\operatorname{supp} \nabla\Psi \subset \{\mathbf{x} \in \mathbb{R}^2 : R_0 < |\mathbf{x}| < R_1\}$
2. $\operatorname{supp}(\nabla + k^2)\omega \subset \{\mathbf{x} \in \mathbb{R}^2 : R_0 < |\mathbf{x}| < R_1\}$.

The first follows directly from the fact that Ψ is in C^2 and constant for $|\mathbf{x}| \leq R_0$ and $|\mathbf{x}| > R_1 > R_0$. The second follows from (2.14) and 1.

In (2.12) we now choose to consider the domain $\Omega = B_R := \{x \in \mathbb{R}^2 : |\mathbf{x}| < R\}$ for $R > 0$. Thus, from (2.12) and Lemma 2.7 we have for $\Omega = B_R$, $R \to \infty$ and $\mathbf{x} > R_1$ the expression

$$u(\mathbf{x}) = -\int_{\operatorname{supp} \nabla\Psi} \Phi(\mathbf{x},\mathbf{y})(2\nabla\Psi \cdot \nabla u + u\Delta\Psi)(\mathbf{y}) d\mathbf{y}. \tag{2.22}$$

By plugging in $\Phi(\mathbf{x},\mathbf{y}) = \frac{e^{ik|\mathbf{x}|}}{\sqrt{|\mathbf{x}|}} \left(C_{d,k} e^{-ik\hat{\mathbf{x}}\cdot\mathbf{y}} + \mathcal{O}\left(\frac{1}{|\mathbf{x}|}\right)\right)$ for $\mathbf{x} \to \infty$, from (2.10) into (2.22) and using *Remark* 2.5 we get

$$u(\mathbf{x}) = -\frac{e^{ik|\mathbf{x}|}}{\sqrt{|\mathbf{x}|}} C_{d,k} \int_{\operatorname{supp} \nabla\Psi} (2\nabla\Psi \cdot \nabla u + u\Delta\Psi)(\mathbf{y}) e^{-ik\hat{\mathbf{x}}\cdot\mathbf{y}} d\mathbf{y}. \tag{2.23}$$

Together with the asymptotic behavior in (2.8), we obtain

$$u^\infty(\mathbf{x}) = -C_{d,k} \int_{\operatorname{supp} \nabla\Psi} (2\nabla\Psi \cdot \nabla u + u\Delta\Psi)(\mathbf{y}) e^{-ik\hat{\mathbf{x}}\cdot\mathbf{y}} d\mathbf{y} \tag{2.24}$$

We can now rewrite (2.24) by employing Green's Theorem and integration by parts. Let $A := \{x \in \mathbb{R}^2 : R_0 < |\mathbf{x}| < R_1\}$ then it holds with *Green's Theorem* (2.1) that

$$\int_A (\nabla\Psi \cdot \nabla u + u\Delta\Psi)(\mathbf{y}) e^{-ik\hat{\mathbf{x}}\cdot\mathbf{y}} d\mathbf{y} = \int_{\partial A} u \frac{\partial \Psi}{\partial \mathbf{n}} dS(y) = 0. \tag{2.25}$$

Since $\frac{\partial \Psi}{\partial \mathbf{n}}|_{\partial A} = 0$. Secondly, we have with integration by parts that

$$\begin{aligned} \int_A (\nabla\Psi \cdot \nabla u) e^{-ik\hat{\mathbf{x}}\cdot\mathbf{y}} d\mathbf{y} &= -\int_A \operatorname{div}(\nabla\Psi \cdot e^{-ik\hat{\mathbf{x}}\cdot\mathbf{y}}) u(\mathbf{y}) d(\mathbf{y}) \\ &\quad + \int_{\partial A} \underbrace{(\nabla\Psi \cdot e^{-ik\hat{\mathbf{x}}\cdot\mathbf{y}} \cdot \mathbf{v}(\mathbf{y}))}_{=0 \text{ since } \nabla\Psi|_{\partial A}=0} u(\mathbf{y}) dS(\mathbf{y}) \\ &= -\int_A (\Delta\Psi - ik\hat{\mathbf{x}}\nabla\Psi) e^{-ik\hat{\mathbf{x}}\cdot\mathbf{y}} u(\mathbf{y}) d\mathbf{y}, \end{aligned} \tag{2.26}$$

Plugging the results from (2.25) and (2.26) into (2.24) gives the desired result

$$\begin{aligned} u^{\infty}(\mathbf{x}) &= -C_{d,k}\left(\int_{\operatorname{supp}\nabla\Psi}(\nabla\Psi\cdot\nabla u + u\Delta\Psi)(\mathbf{y})e^{-ik\hat{\mathbf{x}}\cdot\mathbf{y}}d\mathbf{y} + \int_{\operatorname{supp}\nabla\Psi}(\nabla\Psi\cdot\nabla u)(\mathbf{y})e^{-ik\hat{\mathbf{x}}\cdot\mathbf{y}}d\mathbf{y}\right) \\ &= C_{d,k}\int_{A}(\Delta\Psi - ik\hat{\mathbf{x}}\nabla\Psi)e^{-k\hat{\mathbf{x}}\cdot\mathbf{y}}u(\mathbf{y})d\mathbf{y} \end{aligned}$$

Note: The constant $C_{d,k}$ we obtained in Example 2.4. □

Chapter 3

Derivation of the Shape-Gradient

The main goal of this Chapter is to derive an expression of the shape derivative of a Shape-functional witch is defined in the next section. To do this, we will first go through the idea of a shape-gradient.

3.1 The Shape-gradient

In this section, we are going to introduce the shape function and define the concept of shape gradient. For this follow ([7] Sect. 2.1, Ch. 2).

3.1.1 Shape Function

To be able to measure shape sensitivity, we define a shape function, the L^2 far-field tracking functional (3.1). The purpose of this is to be able to measure the difference between our reference solution from the far-field pattern and our measured scattered pattern. Therefore, we define our shape function as,

$$J(u(D)) = ||u_g - u_\infty(D)||^2_{L^2(\mathbb{S}^1)} = \int_{\mathbb{S}^1} |u_g - u_\infty(D)|^2 d\mathbb{S}. \tag{3.1}$$

In this expression, $u_g \in L^2(\mathbb{S}^1)$ represents the measured data of the scattered wave, and $u_\infty(D)$ is our actual far-field pattern for our shape D satisfying the boundary value problem (1.2) and (1.3).

3.1.2 Shape Gradient

Shape sensitivity is defined as the impact of small perturbation of the shape on our shape function $J(D)$. To be able to model the perturbation, we will introduce the following map

$$\Phi_s(\mathbf{x}) = \mathbf{x} + s\mathcal{V}(\mathbf{x}),\ \mathbf{x} \in \mathbb{R}^2, \tag{3.2}$$

where $\mathcal{V} : \mathbb{R}^2 \to \mathbb{R}^2$ is a smooth vector-field in $\mathbb{R}^2$. We notice that by using the mapping (3.2), it is natural to consider $J(D)$ as a mapping

$$J : \mathcal{U}_{ad} \to \mathbb{R}, \tag{3.3}$$

where $\mathcal{U}_{ad}$ is defined as the family of admissible domains

$$\mathcal{U}_{ad} := \{\Phi_s(\mathbf{x}) | \mathbf{x} \in C^1(\Omega)\}. \tag{3.4}$$

The sensitivity can then be expressed as the derivative of the shape functional J in the direction $\mathcal{V}$. More precisely, that is

$$\boxed{\left\langle \frac{dJ(D)}{dD}, \mathcal{V} \right\rangle := \lim_{s \to 0} \frac{J(D_s) - J(D)}{s},} \tag{3.5}$$

where we have used the notation $D_s := \Phi_s(D)$.

It is necessary to investigate different ways to compute this derivative.

3.2 Derivative of the Shape Gradient

To derive the shape gradient, we could simply derive our shape function (3.1). We would then with the chain rule obtain the expression

$$\left\langle \frac{dJ(u(D))}{du}, \langle u'(D), \mathcal{V} \rangle \right\rangle, \tag{3.6}$$

where $\frac{dJ(u(D))}{du}$ is the derivative of the functional J with respect to u and $\langle u'(D), \mathcal{V} \rangle$ is the derivative of u with respect to the perturbation in the direction of $\mathcal{V}$,

$$\langle u'(D), \mathcal{V} \rangle = \left. \frac{du}{ds} \right|_{s=0}.$$

Calculating the derivative like this leaves us with an equivalent problem for each coordinate of the Domain Ω. In the next section, to avoid this, we are going to use a different approach.

3.3 Adjoint method

In the following, instead of calculating the derivative directly, we will now introduce a new approach and more efficient way of representing the derivative. We will namely derive the shape gradient of our shape functional (3.1) with an adjoint method using a Lagrangian approach. A lot of the work is similar to the one done in ([7] Sect. 2.1, Ch. 2).

Theorem 3.1. *Let D be a long shaped simply connected planar domain with analytic boundary ∂D and let $\Omega = \mathbb{R}^2 \setminus \bar{D}$. The shape derivative of the shape functional (3.1) constrained to (1.2) and (1.3) reads*

$$\left\langle \frac{dJ(\Omega)}{dD}, \mathcal{V} \right\rangle = \int_\Omega \nabla u(div\mathcal{V} - D\mathcal{V} - D\mathcal{V}^T)\nabla v - k^2 uv\, div\mathcal{V} dx. \tag{3.7}$$

and can be recast to a boundary integral as

$$\left\langle \frac{dJ(D)}{dD}, \mathcal{V} \right\rangle = \int_{\partial\Omega} \mathcal{V} \cdot \mathbf{n}(\nabla u \nabla v) dS, \tag{3.8}$$

where $v \in H^1_{\partial D}(\Omega)$ is the solution of the corresponding adjoint problem:

$$2\int_{\mathbb{S}^1} (F(u) - u_g)F(\phi) d\mathbb{S} - \int_\Omega -\nabla\phi \cdot \nabla v - k^2 \phi v d\mathbf{x} + \int_{\partial\Omega^*} v\nabla\phi \cdot \mathbf{n} dS = 0,$$

for all $\phi \in H^1_{\partial D}(\Omega)$. $F(u)(x)$ is the volume representation of the far-field function.

Proof. To compute the derivative, it is convenient to work with the variational formulation (1.5) introduced in the introduction. As explained in (3.1.2) we induced the map $\Phi_s(x) = x + s\mathcal{V}$ to be able to model a small perturbation of our obstacle, which then is used to express the derivative. By employing transformation techniques on the variational formulation (1.5), we can get rid of the parameter s from the integral domain $\Omega_s := \Phi(\Omega)$ ([8] Sect. 4.1-3, Ch. 9). Accordingly, the variational constraints can be equivalently formulated as

$$a : \mathbb{R} \times H^1_{\partial D}(\Omega) \times H^1_{\partial D}(\Omega) \to \mathbb{R}, \quad a = a(s; u, v),$$

where

$$\begin{aligned} a(s; u, v) &= \int_{\Omega_s} -\nabla u \cdot \nabla v - k^2 uv dx + \int_{\partial\Omega^*} Dt\mathcal{N}_k(u|_{\partial\Omega^*})v|_{\partial\Omega^*} dS \\ &= \int_\Omega -\nabla(u \circ \Phi_s) \cdot \nabla(v \circ \Phi_s) D\Phi_s^{-1} D\Phi_s^{-T} \\ &\quad - k^2 (u \circ \Phi_s)(v \circ \Phi_s) \det D\Phi_s d\mathbf{x} + \int_{\partial\Omega^*} Dt\mathcal{N}_k(u|_{\partial\Omega^*})v|_{\partial\Omega^*} dS, \end{aligned} \tag{3.9}$$

for all $u, v \in H^1_{\partial D}(\Omega)$ and with $\Omega_s := \mathbb{R}^2 \setminus \bar{D}_s$. We have that $u(\Phi_s(x)) := (u \circ \Phi_s)(x)$. By setting $u(\mathbf{x}') = u(\Phi_s(x))$ and renaming $v := (v \circ \Phi_s)$, (3.9) is

equivalent to

$$a(s;u,v) = \int_\Omega (-\nabla u(\mathbf{x}') \cdot \nabla v(\mathbf{x}') D\Phi_s^{-1} D\Phi_s^{-T} - k^2 u(\mathbf{x}')v(\mathbf{x}')) \det D\Phi_s d\mathbf{x}' + \int_{\partial\Omega^*} Dt\mathcal{N}(u|_{\partial\Omega^*})v|_{\partial\Omega^*} dS. \tag{3.10}$$

for all $u, v \in H^1_{\partial D}(\Omega)$ and with $D\Phi_s^{-1} = (D\Phi_s(\mathbf{x}'))^{-1}$. We notice that the second term of $a(u,v)$ and $l(v)$ is not affected by the transformation, as the truncation boundary is by definition not affected by the deformation of D, that is $\Phi_\mathcal{V}|_{\partial\Omega^*} = \mathbf{I}$. Hence we simply have

$$\begin{aligned} &l : \mathbb{R} \times H^1_{\partial D}(\Omega) \to \mathbb{R}, \quad l = l(s;v) \\ &l(s;v) = \int_{\partial\Omega^*} (-\gamma_N u^{inc} + Dt\mathcal{N}_k(u^{inc}|_{\partial\Omega^*}))v|_{\partial\Omega^*} dS, \end{aligned} \tag{3.11}$$

for all $v \in H^1_{\partial D}(\Omega)$. We can use (3.10) and (3.11) to replace the constraints (1.2) with a parameter dependent variational problem:

$$a(s;u,v) = l(s;v),$$

where a and l is as in (3.10) and (3.11). Note that our shape functional

$$\begin{aligned} &J : \mathbb{R} \times H^1_{\partial D}(\Omega) \to \mathbb{R} \quad J = J(s;u(s)) \\ &J(s;u(s)) = ||u_g - F(u)||^2_{L^2(\mathbb{S}^1)} \end{aligned}$$

as well as a and l "only" indirectly depends on the parameter s. $F(u)$ is the volume representation of the far-field and linear in $u \in H^1_{\partial D}(\Omega)$.

It is now convenient to define the following bilinear form

$$e(s;u,v) = a(s;u,v) - l(s;v). \tag{3.12}$$

Now we choose to introduce the Lagrangian

$$\begin{aligned} &\mathcal{L} : \mathbb{R} \times H^1_{\partial D}(\Omega) \times H^1_{\partial D}(\Omega) \to \mathbb{R}, \\ &\mathcal{L}(s;u,v) = J(s;u) - e(s;u,v) = J(s;u) - [a(s;u,v) - l(s;v)]. \end{aligned} \tag{3.13}$$

We can write

$$\mathcal{L}(s;u,v) = J(s;u)$$

as $e(s;u,v) = 0$ for all $v \in H^1_{\partial D}(\Omega)$ when the variational constrains are satisfied. Therefore, we can compute the shape derivative as follows

$$\left\langle \frac{dJ(D)}{dD}, \mathcal{V} \right\rangle = \lim_{s\to 0} \frac{J(D_s) - J(D)}{s} = \lim_{s\to 0} \frac{\mathcal{L}(s;u(s),v) - \mathcal{L}(s;u(0),v)}{s}. \tag{3.14}$$

This reads,

$$\left.\frac{d\mathcal{L}(s;u(s),v)}{ds}\right|_{s=0} = \frac{d\mathcal{L}(s;u(s),v)}{\partial s} + \left\langle \frac{d\mathcal{L}(s;u(s),v)}{\partial u}, \left.\frac{du}{ds}\right|_{s=0} \right\rangle$$

The Lagrange multiplier v is a free parameter in $H^1_{\partial D(\Omega)}$. We choose v in a way, such that, $\langle \partial_u \mathcal{L}, \phi \rangle = 0$ to avoid having to compute

$$\left.\frac{du}{ds}\right|_{s=0}.$$

This leaves us with the adjoint equation

$$\left\langle \frac{d\mathcal{L}(s;u(s),v)}{\partial u}, \phi \right\rangle = 0, \quad \text{for all } \phi \in H^1_{\partial D(\Omega)}. \tag{3.15}$$

That is

$$2\int_{\mathbb{S}^1} (F(u) - u_g)F(\phi)d\mathbb{S} - \int_\Omega -\nabla\phi\cdot\nabla v - k^2\phi v d\mathbf{x} + \int_{\partial\Omega^*} v\nabla\phi\cdot\mathbf{n}dS = 0, \tag{3.16}$$

for all $\phi \in H^1_{\partial D(\Omega)}$. When v is chosen this way, the expression (3.14) simplifies to

$$\left\langle \frac{dJ(D)}{dD}, \mathcal{V} \right\rangle = \underbrace{\frac{\partial J(s;u(s),v)}{\partial s}}_{①} - \underbrace{\frac{\partial a(s;u(s),v)}{\partial s}}_{②} + \underbrace{\frac{\partial l(s;u(s),v)}{\partial s}}_{③}. \tag{3.17}$$

We will now derive the explicit form of the shape gradient. The partial derivatives on the right-hand side of (3.17) can be computed by employing transformation techniques. We will start with the first term ① :

We conclude, with the chain rule, that the partial derivative must equal zero. As the shape functional $||u_g - F(u)||^2_{L^2(\mathbb{S}^1)}$ does not directly depend on s, specifically

$$\frac{\partial J(s;u(s),v)}{\partial s} = 2\int_{\mathbb{S}^1} (F(u) - u_g)d\mathbb{S}\cdot \underbrace{\frac{F(u)}{\partial s}}_{=0} = 0. \tag{3.18}$$

Before we start deriving the second term ② of (3.17) we are going to show two identities.

Lemma 3.2. *For $D\Phi_s$ being the Jacobian matrix of Φ_s, It holds,*

1. $\det(D\Phi_s) = 1 + div(s\mathcal{V}) + \mathcal{O}(||s\mathcal{V}||)$
2. $D\Phi_s^{-1} = \mathbf{I} - D(s\mathcal{V}) + \mathcal{O}(||s\mathcal{V}||^2_{C^1})$.

Proof (2D-case). 1. We start with the first identity. It holds that

$$D\Phi_s := \begin{bmatrix} \frac{\partial \Phi_{s1}}{\partial \mathbf{x}_1} & \frac{\partial \Phi_{s1}}{\partial \mathbf{x}_2} \\ \frac{\partial \Phi_{s2}}{\partial \mathbf{x}_1} & \frac{\partial \Phi_{s2}}{\partial \mathbf{x}_2} \end{bmatrix} = \begin{bmatrix} 1 + s\frac{\partial \mathcal{V}_1(\mathbf{x})}{\partial \mathbf{x}_1} & s\frac{\partial \mathcal{V}_1(\mathbf{x})}{\partial \mathbf{x}_2} \\ s\frac{\partial \mathcal{V}_2(\mathbf{x})}{\partial \mathbf{x}_1} & 1 + s\frac{\partial \mathcal{V}_2(\mathbf{x})}{\partial \mathbf{x}_2} \end{bmatrix}$$

Then we have that

$$\begin{aligned} \det(D\Phi_s) &= (1 + s\frac{\partial \mathcal{V}_1(\mathbf{x})}{\partial \mathbf{x}_1}) \cdot (1 + s\frac{\partial \mathcal{V}_2(\mathbf{x})}{\partial \mathbf{x}_2}) - s\frac{\partial \mathcal{V}_1(\mathbf{x})}{\partial \mathbf{x}_2} \cdot s\frac{\partial \mathcal{V}_2(\mathbf{x})}{\partial \mathbf{x}_1} \\ &= 1 + \underbrace{s\frac{\partial \mathcal{V}_2(\mathbf{x})}{\partial \mathbf{x}_1} + s\frac{\partial \mathcal{V}_1(\mathbf{x})}{\partial \mathbf{x}_2}}_{\mathrm{div} s\mathcal{V}} + \underbrace{s\frac{\partial \mathcal{V}_1(\mathbf{x})}{\partial \mathbf{x}_1} \cdot s\frac{\partial \mathcal{V}_2(\mathbf{x})}{\partial \mathbf{x}_2} - s\frac{\partial \mathcal{V}_1(\mathbf{x})}{\partial \mathbf{x}_2} \cdot s\frac{\partial \mathcal{V}_2(\mathbf{x})}{\partial \mathbf{x}_1}}_{\mathcal{O}(||s\mathcal{V}||)} \end{aligned}$$

2. For the following equalities, we use the fact that $(1+s\mathcal{V}_i)^{-1} = \sum_{k\geq 0}(-1)^k(s\mathcal{V}_i)^k$ when s small enough and $i \in \{1, 2\}$.

$$\begin{aligned} D\Phi_s^{-1} &:= \begin{bmatrix} \frac{\partial \Phi_{s1}^{-1}}{\partial \mathbf{x}_1} & \frac{\partial \Phi_{s1}^{-1}}{\partial \mathbf{x}_2} \\ \frac{\partial \Phi_{s2}^{-1}}{\partial \mathbf{x}_1} & \frac{\partial \Phi_{s2}^{-1}}{\partial \mathbf{x}_2} \end{bmatrix} = \begin{bmatrix} 1 + \sum_{k\geq 1}(-1)^k s^k \frac{\partial \mathcal{V}_1^k(\mathbf{x})}{\partial \mathbf{x}_1} & \sum_{k\geq 1}(-1)^k s^k \frac{\partial \mathcal{V}_1^k(\mathbf{x})}{\partial \mathbf{x}_2} \\ \sum_{k\geq 1}(-1)^k s^k \frac{\partial \mathcal{V}_2^k(\mathbf{x})}{\partial \mathbf{x}_1} & 1 + \sum_{k\geq 1}(-1)^k s^k \frac{\partial \mathcal{V}_2^k(\mathbf{x})}{\partial \mathbf{x}_2} \end{bmatrix} \\ &= \mathbf{I} - D(s\mathcal{V}) + \mathcal{O}(||s\mathcal{V}||_{C^1}^2). \end{aligned}$$

□

Remark 3.3. This proof can easily be generalized to n-dimension.

By plugging in the identities from Lemma 3.2 in (3.10), it becomes clear that

$$\frac{\partial a(s; u(s), v)}{\partial s} = \int_\Omega -\nabla u(\mathrm{div}\mathcal{V} \cdot \mathbf{I} - D\mathcal{V} - D\mathcal{V}^T)\nabla v + k^2 uv\mathrm{div}\mathcal{V} dx. \tag{3.19}$$

The derivative of the second term in (3.10) vanishes, as it does not directly depend on s. More precisely, the Dirchet-to-Neumann operator is linear, and the truncation boundary is not affected by the vector-field deformation and therefore does not depend on s. The partial derivative with respect to s is therefore zero.

For the third term, ③ in (3.17) we also have that it does not directly depend on s and is equal to zero.

Using (3.17) as well as the results in (3.18) and (3.19) we can compute the shape derivative, and we get

$$\boxed{\left\langle \frac{dJ(\Omega)}{dD}, \mathcal{V} \right\rangle = \int_\Omega \nabla u(\mathrm{div}\mathcal{V} \cdot \mathbf{I} - D\mathcal{V} - D\mathcal{V}^T)\nabla v - k^2 uv\mathrm{div}\mathcal{V} dx.}$$

Which correspond to the formula (3.7).

Boundary representation of the shape derivative

The main goal of this section of the proof is to recast the shape derivative (3.7) to a boundary integral of the form

$$\int_{\partial\Omega} f(x)\ \mathcal{V}\cdot\mathbf{n}(x)dS. \tag{3.20}$$

Here again we work similarly to ([7] Ch. 2, Sect. 2.1). To start with, we choose to rewrite (3.7) as

$$\int_{\Omega} -\nabla u(D\mathcal{V}+D\mathcal{V}^T)\nabla v + \mathrm{div}\mathcal{V}(\nabla u\nabla v - k^2uv)dx. \tag{3.21}$$

We consider the following result,

Theorem 3.4 (Regularity Theorem)**.** [1] *Let a be an H_0^1-elliptic bilinear form with sufficient smooth coefficient functions.*

1. *If Ω is convex, then the Dirichlet problem is H^2-regular*
2. *If Ω has a C^s boundary with $s\geq 2$, then the Dirchlet problem is H^s-regular*

As a consequence of Theorem, 3.4, we have that the solution of u and v are in $H^2(\Omega)$. We can therefore imply the following vector identity ([10], Sect. 6, id. 43):

$$\begin{aligned}\mathcal{V}\cdot\nabla(\nabla u\cdot\nabla v)+\nabla u(D\mathcal{V}+D\mathcal{V}^T)\nabla v &= \nabla(\mathcal{V}\cdot\nabla u)\cdot\nabla v+\nabla u\cdot\nabla(\mathcal{V}\cdot\nabla v)\\ \iff -\nabla u(D\mathcal{V}+D\mathcal{V}^T)\nabla v &= -\nabla(\mathcal{V}\cdot\nabla u)\cdot\nabla v-\nabla u\cdot\nabla(\mathcal{V}\cdot\nabla v)\\ &\quad +\mathcal{V}\cdot\nabla(\nabla u\cdot\nabla v).\end{aligned} \tag{3.22}$$

Substituting (3.22) into (3.21) results in

$$\left\langle\frac{dJ(D)}{dD},\mathcal{V}\right\rangle = \int_{\Omega} -\nabla(\mathcal{V}\cdot\nabla u)\cdot\nabla v-\nabla u\cdot\nabla(\mathcal{V}\cdot\nabla v)+\underbrace{\mathrm{div}\mathcal{V}(\nabla u\nabla v-k^2uv)}_{①}dx. \tag{3.23}$$

By the linearity and the product rule, it holds that ① can be rewritten as follows,

$$\begin{aligned}\mathrm{div}(\mathcal{V}(\nabla u\nabla v-k^2uv) &\overset{lin.}{=} \mathrm{div}(\mathcal{V}(\nabla u\nabla v))-\mathrm{div}(\mathcal{V}(k^2uv))\\ &\overset{prod.}{=} \mathrm{div}(\mathcal{V})(\nabla u\nabla v)+\nabla(\nabla u\nabla v)\mathcal{V}-\mathcal{V}\cdot(k^2\nabla(u)+k^2\nabla(v)u)\\ &\quad -\mathrm{div}(\mathcal{V})(k^2uv).\end{aligned}$$

[1] The theorem is taken from ([9] Ch. 2, Thm 2.2)

Thus,

$$\begin{aligned}\operatorname{div}(\mathcal{V})(\nabla u \nabla v - k^2 uv)) = \operatorname{div}(\mathcal{V}(\nabla u \nabla v - k^2 uv) - \nabla(\nabla u \nabla v)\mathcal{V}) \\ + \mathcal{V} \cdot (k^2 \nabla(u)v + k^2 \nabla(v)u).\end{aligned} \tag{3.24}$$

Substituting (3.24) into (3.23) leaves us with the expression

$$\begin{aligned}\left\langle \frac{dJ(D)}{dD}, \mathcal{V} \right\rangle = \int_\Omega -\nabla(\mathcal{V} \cdot \nabla u) \cdot \nabla v - \nabla u \cdot \nabla(\mathcal{V} \cdot \nabla v) \\ + \operatorname{div}(\mathcal{V}(\nabla u \nabla v - k^2 uv)) + \mathcal{V} \cdot (k^2 \nabla(u)v + k^2 \nabla(v)u) dx.\end{aligned}$$

After rearranging the terms, we are left with the sum of the following next three integrals

$$\left\langle \frac{dJ(D)}{dD}, \mathcal{V} \right\rangle = \int_\Omega \operatorname{div}(\mathcal{V}(\nabla u \nabla v - k^2 uv)) \tag{3.25}$$

$$+ \int_\Omega \nabla u \cdot \nabla(\mathcal{V} \cdot \nabla v) + u k^2 \mathcal{V} \cdot \nabla v \tag{3.26}$$

$$+ \int_\Omega -\nabla v \cdot \nabla(\mathcal{V} \cdot \nabla u) + v k^2 \mathcal{V} \cdot \nabla u. \tag{3.27}$$

The goal is now to write these three integrals as a boundary integral. Starting with the first one, we have with Gauss divergence theorem that

$$\int_\Omega \operatorname{div}(\mathcal{V}(\nabla u \nabla v - k^2 uv) = \int_{\partial\Omega} \mathcal{V} \cdot \mathbf{n}(\nabla u \nabla v - k^2 uv) dS.$$

For the second integral, we have that it has to equal zero due to the state equation or the variational constrains (1.2) and (1.5). In detail, we have that

$$a(s, u, v) = l(v) \quad \forall\, v \in H^1(\Omega)_{\partial D} = \{w \in H^1(\Omega) : w|_{\partial D} = 0\}.$$

Moreover, $\mathcal{V} \cdot \nabla v \in H^1_{\partial D}(\Omega)$ as $v \in H^1_{\partial D}(\Omega)$ and $\mathcal{V} \in C^\infty(\Omega) \subset H^1(\Omega)$. Plugging this into (1.5) leaves us with

$$\int_\Omega \nabla u \cdot \nabla(\mathcal{V} \cdot \nabla v) + u k^2 \mathcal{V} \cdot \nabla v = 0,$$

as $\mathcal{V} = 0$ on the truncation boundary $\partial\Omega^*$.

Lastly, due to the adjoint equation (3.16), the third equation must as well equal zero. More precisely, we have again that $\mathcal{V} \cdot \nabla u \in H^1_{(\partial D)}(\Omega)$ as $u \in H^1_{\partial D}(\Omega)$ and $\mathcal{V} \in C^\infty(\Omega) \subset H^1(\Omega)$, as well as the adjoint equation

$$2 \int_{\mathbb{S}^1} (F(u) - u_g) F(\phi) d\mathbb{S} - \int_\Omega -\nabla\phi \cdot \nabla v - k^2 \phi v = - \int_{\partial\Omega^*} v \nabla\phi \cdot \mathbf{n} dS \quad \forall\, \phi \in H^1_{\partial D}(\Omega), \tag{3.28}$$

As (3.28) holds for any $\phi \in H^1_{\partial D}(\Omega)$, we can therefore choose $\phi = \mathcal{V} \cdot \nabla u \in H^1_{\partial D}(\Omega)$. Then the first integral in (3.28) vanishes as $\mathcal{V} = 0$ on the integration domain A of the far-field function, F . For the right-hand side of (3.28), we again have that $\mathcal{V} = 0$ on the truncation boundary, $\partial\Omega^*$ and therefore the integral must equal zero. We therefore end up with

$$\int_\Omega -\nabla v \cdot \nabla(\mathcal{V} \cdot \nabla u) + vk^2 \mathcal{V} \cdot \nabla u = 0.$$

For the shape derivative, we find

$$\left\langle \frac{dJ(D)}{dD}, \mathcal{V} \right\rangle = \int_{\partial\Omega} \mathcal{V} \cdot \mathbf{n}(\nabla u \nabla v) dS - \int_{\partial\Omega} \mathcal{V} \cdot \mathbf{n}(k^2 uv) dS. \tag{3.29}$$

From (1.2) we have that $u = 0$ on $\partial\Omega$. Thus,

$$\boxed{\left\langle \frac{dJ(D)}{dD}, \mathcal{V} \right\rangle = \int_{\partial\Omega} \mathcal{V} \cdot \mathbf{n}(\nabla u \nabla v) dS.}$$

Which correspond to the formula (3.8). *Note: k enters (3.8) through the state equation and the adjoint equation*

□

Chapter 4

The Method of Fundamental Solution

In this chapter, we are going to investigate another method of deciding the shape sensitivity of D with the help of the Method of Fundamental solution (MFS). In which we approximate the solution u of the Helmholtz boundary value problem by fundamental solutions of the Helmholtz equation. The point of this is then that we get a discretized version of the solution [11].

4.1 The Method of Fundamental Solutions for scattering problems

We consider our original boundary value problem, which was presented in the introduction.

$$\begin{cases} \Delta u + k^2 u = 0 & \text{in } \Omega \\ u = 0 & \text{on } \partial\Omega, \end{cases} \tag{4.1}$$

where $u = u_s + u_{inc}$. This can equivalently be written as

$$\begin{cases} \Delta u_s + k^2 u_s = 0 & \text{in } \Omega \\ u_s = -u_{inc} & \text{on } \partial\Omega. \end{cases} \tag{4.2}$$

The idea of the Fundamental solution is to approximate the solution u_s by a linear combination of fundamental solutions in terms of source points $\mathbf{y}_j$ with $j \in \{1, ..., n\}$ equispaced on a closed source curve Σ contained in inside the domain $D = \mathbb{R}^2 \setminus \Omega$. Thus,

$$\boxed{u_s(\mathbf{x}) \approx u_s^{(n)}(\mathbf{x}) = \sum_{j=1}^{n} \mathbf{c}_j \Phi_k(||\mathbf{x} - \mathbf{y}_j||),\ \mathbf{c}_j \in \mathbb{C},} \tag{4.3}$$

with $\Phi_k(r) = \frac{i}{4}H_0^{(1)}(kr)$ being the fundamental solution of the Helmholtz equation, $H_0^{(1)}$ the Hankel function of the first kind of order zero and n the number of approximating functions, each of which is associated with a source point $\mathbf{y}_j$.

As mentioned in Chapter 2, $\mathbf{x} \to \Phi_k(||\mathbf{x} - \mathbf{y}||)$ is a radiating solution to the Helmholtz equation for any $\mathbf{y} \in \partial D$. This holds because $\mathbf{x} \neq \mathbf{y}$, as one of the points is in the interior of our shape D and the other one is on the boundary ∂D. From this, we conclude that the linear combination also has to be a radiating solution to the Helmholtz equation.

The MFS unknown coefficient $\mathbf{c}_j$ is determined by collocating the boundary condition at m points. For this, we choose $\mathbf{p}_i \in D$, $i \in \{1, ..., m\}$ equidistant, with $m \geq n$. This leads to a linear system of equation

$$\sum_{j=1}^{n} \mathbf{c}_j \underbrace{\Phi_k(||\mathbf{p}_i - \mathbf{y}_j||)}_{A_{ij}} = -u_{inc}(\mathbf{p}_i),\ \mathbf{c}_j \in \mathbb{C}. \tag{4.4}$$

This can be written as

$$\mathbf{Ac} = -\mathbf{u_{inc}},$$

where $\mathbf{A}$ is a $m \times n$ Matrix, $\mathbf{c}$ is an unknown $n \times 1$ vector containing the coefficient $\mathbf{c}_j$ and $\mathbf{u_{inc}}$ is a known $m \times 1$ vector containing the points $u_{inc}(\mathbf{p}_i)$.

As the system is over-determined, we can for example solve it with help of the truncated singular decomposition or QR-decompstion.

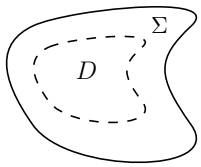

Figure 4.1: closed source curve inside D

4.1.1 Structure of algorithm in 2D

In this section, we are going to approximate source density in finite-dimensional space with a collocational approach.

First, let us take a look at the continuous version of (4.3) and the exact-description of u_s, where instead of considering a vector of coefficients $\mathbf{c}_j$, we have an unknown source density $\varphi(\mathbf{y})$,

$$u_s(x) = \int_\Sigma \Phi_k(||\mathbf{x} - \mathbf{y}||\varphi(\mathbf{y})dS(\mathbf{y}) \stackrel{!}{=} -u_{inc}(\mathbf{x}). \tag{4.5}$$

To approximate the source density we want to minimize the least square

$$|| \int_{\Sigma} \Phi_k(||\mathbf{x}-\mathbf{y}||)\varphi(\mathbf{y})dS(\mathbf{y}) + u_{inc}(\mathbf{x})||^2_{L^2(\partial D)} \tag{4.6}$$

$$= \int_{\partial D} \left| \left(\int_{\Sigma} \Phi_k(||\mathbf{x}-\mathbf{y}||\varphi(\mathbf{y})dS(y) + u_{inc}(\mathbf{x}) \right) \right|^2 dS(\mathbf{x}). \tag{4.7}$$

To be able to do this numerically, we choose to do this on a finite dimensional space and to be able to compute $||\cdot||^2_{L^2(\partial D)}$ we will consider numerical quadrature. More precisely, by considering an n-dimensional space we write

$$\sum_{i=1}^{m} \omega_k \left| \left(\int_{\Sigma} \Phi_k(||\mathbf{p}_i-\mathbf{y}||\varphi(\mathbf{y})dS(\mathbf{y}) + u_{inc}(\mathbf{p}_i) \right) \right|^2$$

$$= \sum_{i=1}^{m} \omega_k \left| \left(\sum_{j=1}^{n} c_j \Phi_k(||\mathbf{p}_i-\mathbf{y}_j||) + u_{inc}(\mathbf{p}_i) \right) \right|^2 .$$

As explained above, a collocation approach is used, meaning that $\mathbf{u}^{(n)}_{inc} = u_{inc}$ on ∂D is enforced in a finite number of points $\mathbf{p}_i, -u_{inc}(\mathbf{p}_i)$. Furthermore, we set all the weights ω_k to equal one, and we become

$$\sum_{i=1}^{m} \left| \left(\sum_{j=1}^{n} \mathbf{c}_j \Phi_k(||\mathbf{p}_i-\mathbf{y}_j||) + u_{inc}(\mathbf{p}_i) \right) \right|^2 . \tag{4.8}$$

Algorithm 1 Find source points

Input: $\mathbf{y}, \mathbf{p}, \mathbf{u_{inc}}$
Output: $\mathbf{c}$
  for $j \in \{1, ..., n\}$ and $i \in \{1, ..., m\}$ **do**
    $(\mathbf{A})_{i,j} \leftarrow \Phi_k(||\mathbf{p}_i - \mathbf{y}_j||)$
  end for
  $\mathbf{c} \leftarrow$ lstsq solution of $\mathbf{Ac} = -\mathbf{u_{inc}}$

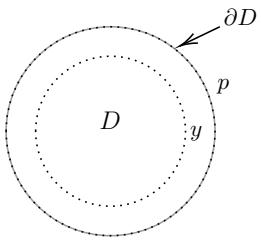

Figure 4.2: closed source curve inside D

Numerical Example - Scattering on unit disk

In this numerical example, we consider D to be a unit disk $D = \{\mathbf{x}; |\mathbf{x}| < 1\}$ centered at the origin. The source points are located inside D on a circle with radius $R = 0.5$ centered at the origin, such that

$$\mathbf{y}_j = Re^{i\phi_j} = (R\cos\phi_j, R\sin\phi_j),\ j = 1, ..., n,$$

with $\phi_j = 2\pi j/n$. The boundary in collocation points is given by

$$\mathbf{p}_i = e^{i\phi_i} = (\cos\phi_i, \sin\phi_i),\ i = 1, ..., m.$$

with $\phi_i = 2\pi i/n$.

The distribution of $\mathbf{y}_j$ and $\mathbf{p}_i$ you can see in figure 4.3:

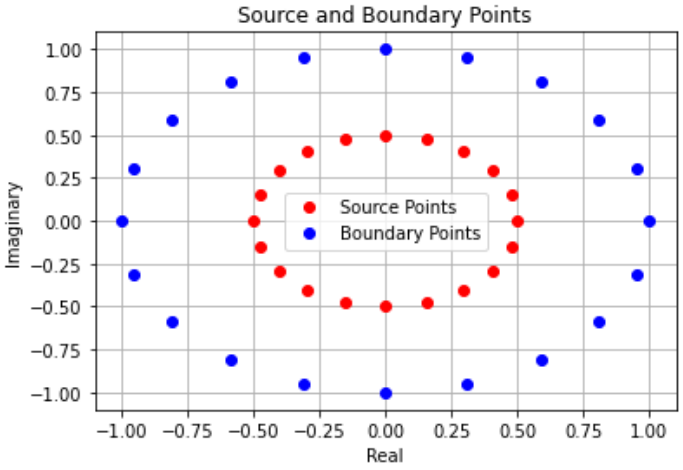

Figure 4.3: Source points and collocation points for n=m=20

In this numerical example, we consider the simplest case of a plane wave with wave number, $k = 1$. Then we can minimize the least square functional (4.8) to obtain the coefficients $\mathbf{c}_j$ and an approximation for u_s. This was accomplished using Python, see appendix I. With the coefficient $\mathbf{c}_j$ in hand, we choose to investigate the convergence of the MFS by plotting the MFS approximation of u_s besides the exact analytical solution of (4.2) which is given by [12]:

$$\begin{aligned} u(r,\theta) =& J_0(kr) - \frac{J_0(ka)H_0^{(1)}(kr)}{H_0^{(1)}(ka)} + 2\sum_{n=1}^{\infty} i^n \cos(n\theta)\left[J_n(kr) - J_n(ka)\frac{H_n^{(1)}(kr)}{H_n^{(1)}(ka)}\right], \\ & (r,\theta) \in \mathbb{R}^2 \setminus B(0;a) = \{r \geq a, \theta \in [0, 2\pi)\} \end{aligned} \tag{4.9}$$

where $k = 1$ and $a = 1$ is the radius of our obstacle. We now choose to plot the real and imaginary parts of our MFS solution for, $m = n \in \{3, 5, 20\}$ on, $x \in B(0, 2)$ besides the exact solution $u_s = u - u_{inc}$ which we obtain with (4.9). By looking at the plots, it would seem that the MFS approximation converges towards the exact solution.

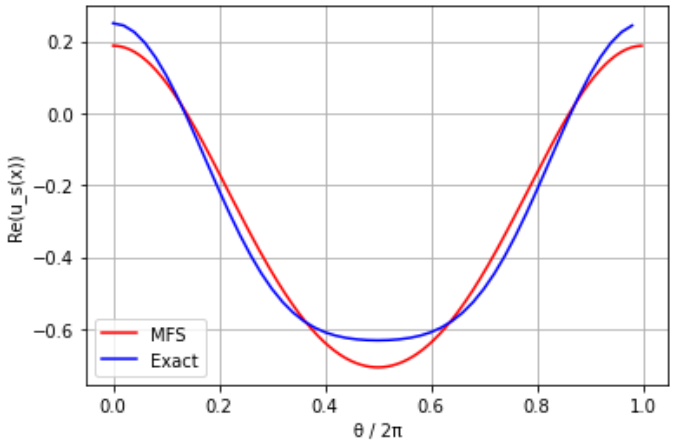

Figure 4.4: Real plot for n=m=3

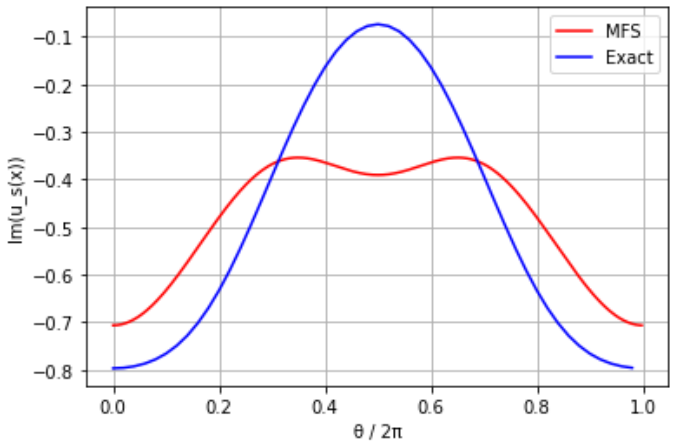

Figure 4.5: Imaginary plot for n=m=3

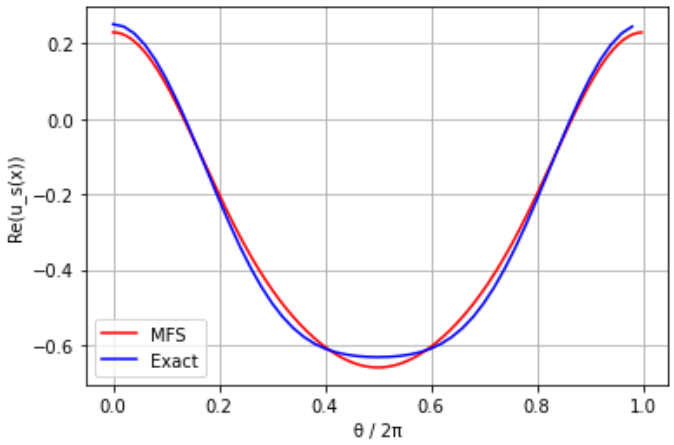

Figure 4.6: Real plot for n=m=5

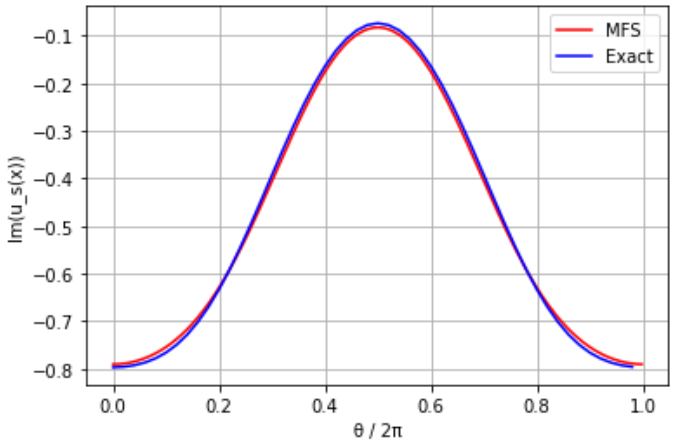

Figure 4.7: Imaginary plot for n=m=5

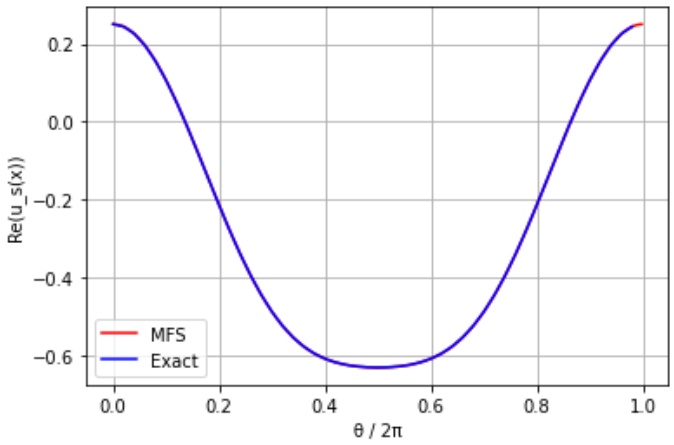

Figure 4.8: Real plot for n=m=20

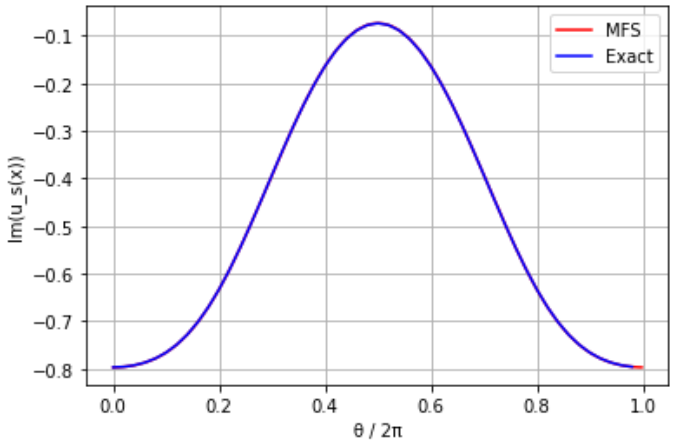

Figure 4.9: Imaginary plot for n=m=20

4.2 Inverse Scattering problem with MFS

In this section, we are going to use the MFS approach to approximate the solutions of the adjoint boundary value problem and derive the derivative formula of our far-field tracking functional J.

Theorem 4.1. *The shape derivative of*

$$J(D,u) = ||u_g - u_\infty(D)||^2_{L^2(\mathbb{S}^1)} = ||u_g - F(u)||^2_{L^2(\mathbb{S}^1)}, \tag{4.10}$$

using the approximation of u_s in (4.3) and where $F(u)(x)$ is the volume representation of the far-field function, can be formulated as

$$\begin{aligned}\left\langle \frac{dJ(D)}{dD}, \mathcal{V} \right\rangle =& \partial_r \Phi(||T(\mathbf{p}_i) - T(\mathbf{y}_j)||) \frac{(T(\mathbf{p}_i) - T(\mathbf{y}_j)) \cdot (\mathcal{V}(\mathbf{p}_i) - \mathcal{V}(\mathbf{y}_j))}{||T(p_k) - T(\mathbf{y}_j)||} \cdot uv \\ &+ \nabla u_{inc}(T(\mathbf{p}_i)) \cdot \mathcal{V}(\mathbf{p}_i) \cdot v,\end{aligned} \tag{4.11}$$

where v is the corresponding solution of the adjoint equation,

$$\left\langle \frac{\partial \mathcal{L}}{\partial u}, \phi \right\rangle = 2 \int_{\mathbb{S}^1} (F(u) - u_g) F(\phi) d\mathbb{S} + \langle \mathbf{A}(D)\phi, v \rangle, \quad \text{for all } \phi \in H^1(\Omega).$$

and

$$\begin{aligned} &T : \mathbb{R}^2 \to \mathbb{R}^2, \ T(\mathbf{x}) = \mathbf{x} + s\mathcal{V} \\ &\mathbf{A}_{ij} = \Phi_k(||T(\mathbf{p}_i) - T(\mathbf{y}_j)||). \end{aligned}$$

Proof. We start by once again considering our functional

$$J(D,u) = ||u_g - u_\infty(D)||^2_{L^2(\mathbb{S}^1)} = ||u_g - F(u)||^2_{L^2(\mathbb{S}^1)}, \tag{4.12}$$

$F(u)(x)$ is the Volume representation of the far-field function, a linear function in $u \in H^1_{\partial D}(\Omega)$. We have that u satisfies the variational constraint, $\mathcal{A}(\partial D, \Sigma)u = \mathbf{b}(\partial D)$, where $\mathcal{A}$ is an operator related to the continuous problem (4.5).

As in the previous chapter, we can define the Lagrangian,

$$\mathcal{L}(D,u,v) = J(u(D),D) + \langle \mathcal{A}(D)u - \mathbf{b}(D), v \rangle,$$

where $v \in \mathbb{C}^n$ is a Lagrange multiplier. We choose v in the same way as in Chapter 3, such that the adjoint equation,

$$\left\langle \frac{\partial \mathcal{L}}{\partial u}, \phi \right\rangle = \left\langle \frac{\partial J(D)}{\partial u}, \phi \right\rangle - \left\langle \frac{\partial e(0,v,u(0)}{\partial u}, \phi \right\rangle = 0 \quad \text{for all } \phi \in H^1(\Omega).$$

This is,

$$\left\langle \frac{\partial \mathcal{L}}{\partial u}, \phi \right\rangle = 2 \int_{\mathbb{S}^1} (F(u) - u_g) F(\phi) d\mathbb{S} + \langle \mathcal{A}(D)\phi, v \rangle, \quad \text{for all } \phi \in H^1(\Omega).$$

hence,

$$\left\langle \frac{dJ(D)}{dD}, \mathcal{V} \right\rangle = \left\langle \frac{d\mathcal{L}(D)}{dD}, \mathcal{V} \right\rangle = \left\langle \left\langle \frac{d\mathcal{A}(D)}{dD}, \mathcal{V} \right\rangle u - \left\langle \frac{d\mathbf{b}(D)}{dD}, \mathcal{V} \right\rangle, v \right\rangle.$$

We remember that we are trying to solve the scattering problem, presented in the introduction, for our scatterer $D := \Phi_s(D_0)$. Therefore, we are going to implement it in terms of pursuing diffeomorphism. Thus, we consider the deformation diffeomorphism

$$T : \mathbb{R}^2 \to \mathbb{R}^2,\ T(\mathbf{x}) = \mathbf{x} + s\mathcal{V}.$$

and the over-determined linear system on equation

$$\sum_{j=1}^{n} \mathbf{c}_j \Phi_k(||\mathbf{x} - T(\mathbf{y}_j)||) = -u_{inc}(T(\mathbf{p}_i)),\ \mathbf{c}_j \in \mathbb{C}.$$

Now in the method of fundamental solution in the discrete case, we consider instead of $\mathcal{A}$ the approximation matrix $\mathbf{A}$, defined as

$$\mathbf{A}_{ij} = \Phi_k(||T(\mathbf{p}_i) - T(\mathbf{y}_j)||).$$

Therefore,

$$\begin{aligned} \mathbf{A}_{ij}(D) &= A_{ij}(T(D_0)) \\ \implies \mathbf{A}_{ij}((T + s\mathcal{V})(D_0)) &= \Phi(||T(\mathbf{p}_i) - T(\mathbf{y}_j) + s(\mathcal{V}(\mathbf{p}_i) - \mathcal{V}(\mathbf{y}_j))||). \end{aligned}$$

Deriving this expression with respect to D leaves us with

$$\begin{aligned} \left\langle \frac{d\mathbf{A}_{ij}(D)}{dD}, \mathcal{V} \right\rangle &= \left. \frac{\partial \mathbf{A}_{i,j}(T + s\mathcal{V})}{\partial s} \right|_{s=0} \\ &= \partial_r \Phi(||T(\mathbf{p}_i) - T(\mathbf{y}_j)||) \frac{(T(\mathbf{p}_i) - T(\mathbf{y}_j)) \cdot (\mathcal{V}(\mathbf{p}_i) - \mathcal{V}(\mathbf{y}_j))}{||T(\mathbf{p}_i)) - T(\mathbf{y}_j)||}. \end{aligned}$$

Furthermore, we have for $\mathbf{b}_i = -u_{inc}(p_k)$ that

$$\left\langle \frac{d\mathbf{b}_i(D)}{dD}, \mathcal{V} \right\rangle = \left. \frac{\partial \mathbf{b}_i(T + s\mathcal{V})}{\partial s} \right|_{s=0} = -\nabla u_{inc}(T(\mathbf{p}_i)) \cdot \mathcal{V}(\mathbf{p}_i).$$

Hence, we get the following expression for the shape derivative

$$\begin{aligned} \left\langle \frac{dJ(D)}{dD}, \mathcal{V} \right\rangle =& \partial_r \Phi(||T(\mathbf{p}_i) - T(\mathbf{y}_j)||) \frac{(T(\mathbf{p}_i) - T(\mathbf{y}_j)) \cdot (\mathcal{V}(\mathbf{p}_i) - \mathcal{V}(\mathbf{y}_j))}{||T(\mathbf{p}_i) - T(\mathbf{y}_j)||} \cdot uv \\ &+ \nabla u_{inc}(T(\mathbf{p}_i)) \cdot \mathcal{V}(\mathbf{p}_i) \cdot v. \end{aligned}$$

Witch corresponds to (4.11). □

Chapter 5

Conclusion and Outlook

The thesis aimed to investigate shape sensitivity for acoustic scattering in two dimension. For this, we first introduced the acoustic model and the far-field function. Although, we specifically focused on computing the shape-derivative of the L2 far-field tracking functional, our shape functional. To do this, we relied on two different methods. Firstly, we used the adjoint method. This was a powerful technique that allowed for the efficient calculation of gradients. It involves solving an equation called the adjoint equation, which we derived from the original problem. By using the adjoint method, we obtained the gradient of the shape functional with respect to the parameter s, in the direction of a vector-field, in a computationally efficient way. Making it particularly useful in applications, where the shape functional is hard to evaluate, as the computation cost is also independent of the parameters that representing our scatterer.

The method of fundamental solution was introduced later on. This method involved solving a system of linear equations by approximating the solution using the fundamental solution of the partial differential equation, the Helmholtz equation. The method of fundamental solution offered several advantages in the sense that it is easy to compute and implement. Lastly, we used this approximation to compute the derivative of the shape functional, which was effective. This would as well be easy to implement and is of meshless nature, which implies that we do not have the concern of mesh constraints.

A further interesting aspect of this problem would be to implement the two methods numerically and compare the accuracy depending on the scatterer.

Bibliography

[1] J. Thorpe, *Elementary topics in differential geometries.* New York, NY: Springer, 2011.

[2] F. Ihlenburg, *Finite element analysis of acoustic scattering.* New York, NY: Springer, 1998.

[3] J. H. Ginsberg, *Acoustics-A Textbook for Engineers and Physicists.* New York, NY: Springer, 2018.

[4] R. K. David Colton, *Inverse Acoustic and Electromagnetic Scattering Theory.* New York, NY: Springer, 2013.

[5] R. Kress, *Integral Equation Methods in Inverse Obstacle Scattering with a Generalized Impedance Boundary Condition. In: Dick, J., Kuo, F., Woźniakowski, H. (eds) Contemporary Computational Mathematics - A Celebration of the 80th Birthday of Ian Sloan.* New York, NY: Springer, 23. May 2018.

[6] F. L. E. Jahnke, F. Emde, "'tafeln höheren funktionen'," 1966.

[7] A. Paganini, "Numerical shape optimization with finite elements," Ph.D. dissertation, ETH Zürich, 2016.

[8] J.-P. Z. M. C. Delfour, *Shape and Geometries.* Philadelphia,PA: Society for Industrial and Applied Mathematics (Siam), 2011.

[9] D. Braess, *Finite Elements.* Cambridge: Cambridge University Press, 2007.

[10] M. Berggren, *A unified discrete–continuous sensitivity analysis method for shape optimization. In Applied and numerical partial differential equation.* New York, NY: Springer, 2010.

[11] T. Barnett, A. H; Betcke, "Stability and convergence of the method of fundamental solutions for helmholtz problem on analytic domains," *J. Comput. Phys. 227*, vol. 227, no. 14, pp. 7003–7026, 2008.

[12] R. K. David Colton, *Integral Equation Methods in Scattering Theory.* New York: Wiley, 1983.

Appendix A

Source Code

A.1 Numerical example

The following code snippets are used for the numerical example in section 4.1.1.

A.1.1 Least square solution of c

This code was used to approximate the coefficient c_j and plot the source and boundary points

```
import numpy as np
from scipy.linalg import lstsq
from scipy.special import hankel1
R=1/2
n=20
m=20

def Phi_k(r):
    return 1j*hankel1(0, r )/4

phi_y = np.linspace(0, 2 * np.pi, n, endpoint=False)
phi_p = np.linspace(0, 2 * np.pi, m, endpoint=False)
y = R * np.exp(1j * phi_y)
p = np.exp(1j * phi_p)

u_inc= np.exp(1j*np.cos(phi_p))

A = np.zeros((m, n), dtype=complex)

for i in range(m):
    for j in range(n):
        A[i, j] = Phi_k(np.abs(p[i] - y[j]))
```

```
c, _, _, _ = lstsq(A, -u_inc)
print("Least squares solution: ", c)

import matplotlib.pyplot as plt


# Plot the source and boundary points
plt.figure()
plt.plot(np.real(y), np.imag(y), 'ro', label='Source Points')
plt.plot(np.real(p), np.imag(p), 'bo', label='Boundary Points')
plt.xlabel('Real')
plt.ylabel('Imaginary')
plt.legend()
plt.title('Source and Boundary Points')
plt.grid(True)

# Show the plots
plt.show()
```

A.1.2 Plots of the scattered wave

Real part

The following code was used to plot the real exact solution of u_s and the real approximation of u_s using MFS.

```
    import numpy as np
import matplotlib.pyplot as plt
from C_numex import c
from C_numex import y
from scipy.special import  jn, hankel1

# Exact solution from Colton and Kress
def u(r, theta, a, k):
    sum_term = 0
    for n in range(1, 100):
        in_term = 1j**n  # Replace with the desired coefficient 'in'
        cos_term = np.cos(n * theta)
        Jn_kr = jn(n, k * r)
        Jn_ka = jn(n, k * a)
        Hn_kr = hankel1(n, k * r)
        Hn_ka = hankel1(n, k * a)
        sum_term += in_term * cos_term * (Jn_kr - Jn_ka * Hn_kr / Hn_ka)
```

```
u_real = jn(0, k * r) - jn(0, k * a) * hankel1(0, k * r) /
hankel1(0, k * a) + 2 * sum_term
    return u_real

def Phi_k(r):
    return 1j*hankel1(0, r )/4

# Generate points on the circle with radius 2
radius = 2.0
k=1
num_points = 500
theta = np.linspace(0, 2 * np.pi, num_points, endpoint=False)
x = radius * np.exp(1j * theta)
u_inc = np.real(np.exp(1j * k * radius * np.cos(theta)))
x_axis = theta / (2 * np.pi)


# Calculate the real part of the numerical solution
u_n_real = np.zeros_like(x)
for j in range(len(c)):
    u_n_real += np.real(c[j] * Phi_k(np.abs(x - y[j])))

# Plot the real part of the numerical solution
plt.figure()
plt.plot(x_axis, u_n_real, 'r-', label='Real(u(x))')
a = 1
k = 1
r=2
num_points = 50
theta = np.linspace(0, 2 * np.pi, num_points, endpoint=False)
x_axis = theta / (2 * np.pi)
u_inc = np.real(np.exp(1j * k * r* np.cos(theta)))



# Evaluate the  real part  of the exact function u_s
#for each theta value
u_real = np.real(u(r, theta, a, k)) - u_inc

plt.plot(x_axis, u_real, color='b', label='Real(u)')

plt.xlabel('   / 2  ')
plt.ylabel('Re(u_s(x))')
```

```
plt.legend()

plt.grid(True)

# Show the plot
plt.show()
```

Imaginary part

The following code was used to plot the imaginary exact solution of u_s and the imaginary approximation of u_s using MFS.

```
import numpy as np
import matplotlib.pyplot as plt
from C_numex import c
from C_numex import y
from scipy.special import  jn, hankel1

# Exact solution from Colton and Kress
def u(r, theta, a, k):
    sum_term = 0
    for n in range(1, 100):
        in_term = 1j**n  # Replace with the desired coefficient 'in'
        cos_term = np.cos(n * theta)
        Jn_kr = jn(n, k * r)
        Jn_ka = jn(n, k * a)
        Hn_kr = hankel1(n, k * r)
        Hn_ka = hankel1(n, k * a)
        sum_term += in_term * cos_term * (Jn_kr - Jn_ka * Hn_kr / Hn_ka)

    u_real = jn(0, k * r) - jn(0, k * a) * hankel1(0, k * r) / hankel1(0,
    return u_real

def Phi_k(r):
    return 1j*hankel1(0, r )/4

# Generate points on the circle with radius 2
radius = 2.0
k=1
num_points = 500
theta = np.linspace(0, 2 * np.pi, num_points, endpoint=False)
x = radius * np.exp(1j * theta)
u_inc = np.imag(np.exp(1j * k * radius * np.cos(theta)))
x_axis = theta / (2 * np.pi)
```

```
# Calculate the real part of the numerical solution
u_n_real = np.zeros_like(x)
for j in range(len(c)):
    u_n_real += np.imag(c[j] * Phi_k(np.abs(x - y[j])))

# Plot the real part of the numerical solution
plt.figure()
plt.plot(x_axis, u_n_real, 'r-', label='MFS')
a = 1
k = 1
r=2
num_points = 50
theta = np.linspace(0, 2 * np.pi, num_points, endpoint=False)
x_axis = theta / (2 * np.pi)
u_inc = np.imag(np.exp(1j * k * r* np.cos(theta)))



# Evaluate the  real part  of the exact function u_s for each theta value
u_real = np.imag(u(r, theta, a, k)) - u_inc

plt.plot(x_axis, u_real, color='b', label='Exact')

plt.xlabel('    / 2   ')
plt.ylabel('Im(u_s(x))')
plt.legend()

plt.grid(True)

# Show the plot
plt.show()
```

A.2 Plot of Hankel function

This code is used to plot the real and imaginary part of the Hankel function of the first kind, order zero in the introduction.

```
# Define the range of values for the independent variable
r = np.linspace(0, 10, 1000)
```

```
# Compute the Hankel function of the first kind, order 0
hankel = hankel1(0, r)

# Plot the real and imaginary parts of the Hankel function
fig, ax = plt.subplots()
ax.plot(r, hankel.real, label='Real part')
ax.plot(r, hankel.imag, label='Imaginary part')
ax.set_xlabel('r')
ax.set_ylabel('Hankel function of the first kind, order 0')
ax.legend()
plt.show()
```